Study on Double Resonant Performance of Air-core Spiral Tesla Transformer Applied in Repetitive Pulsed Operation

Lee Li[1,3], Ma Ning[1], Chen Dehuai[2], Liu Lun[1], Kang Qiang[2], Li Mingjia[2], Cheng Yong[1] and Pan Yuan[1,3]

[1] State Key Laboratory of Advanced Electromagnetic Engineering and Technology
School of electrical & electronic engineering, Huazhong University of Science and Technology
Wuhan, 430074, P.R. China
[2] China Academy of Engineering Physics, Mianyang, 621900, P.R. China
[3] IFSA Collaborative Innovation Center, Shanghai Jiao Tong University
Shanghai, 200240, P.R. China

ABSTRACT

Air-core Tesla transformer combined with semiconductor devices can generate repetitive high-voltage pulses effectively. Air-core Tesla transformer of spiral type is suitable for repetitive operation since its primary voltage is relatively low. Based on the double resonance circuit of air-core Tesla transformer, the expressions of secondary voltage, primary current, and the maximum rise-rate of primary current are deduced. The effects of tuning characteristic on the output voltage and energy efficiency are simulated, and further verified by experiments. An air-core Tesla transformer prototype of spiral type is developed. To achieve repetitive operation, a resonant charging and discharging circuit based on air-core Tesla transformer is designed. The repetitive system based on this prototype can generate microsecond pulses with an average peak voltage of -140 kV at 300 Hz repetition rate. In repetitive mode, the tuning ratio is recommended to range in 1.0-2.0 to achieve high energy efficiency. The output voltage could be higher by increasing the charging voltage or tuning ratio.

Index Terms - **Air-core Tesla transformer, resonant charging, tuning ratio, secondary voltage, energy efficiency.**

1 INTRODUCTION

THE rapidly developing pulsed power technology and high-voltage pulsed generators have been widely applied in many fields such as electron beam accelerators, gas discharge plasma, ultra bandwidth (UWB) systems, dielectric material researches, etc [1-7]. Traditional pulse generators cannot meet the requirements of high voltage, high repetition rate and fast rise-time any more [8].The development of high performance pulsed power generators has become a hot spot in the field of pulsed power technology [12, 13]. Tesla transformer has large application potential among different high-voltage pulse transformers. Tesla transformer combined with pulse capacitors is a common technical proposal to generate high-pulsed voltage. The most representative applications of Tesla transformer are the SINUS-series and RADAN-series accelerators in Russia [9, 10]. The TPG-series accelerators in China are also based on Tesla transformer [11].

Magnetic-core transformer has high coupling coefficient and high energy efficiency. But the transformer of this type is affected by the saturation of ferromagnetic materials. The core loss may be high. So the pulse amplitude and the repetition rate are still limited. Tesla transformer with open magnetic-core has high coupling coefficient and high energy efficiency [9, 10]. The size of magnetic-core Tesla transformer is small. But the transformer of this type has complicate structure, and the insulation between the magnetic core and the windings is a difficult problem. Compared with above transformers, air-core Tesla transformer has no magnetic core; its magnetizing inductance and the coupling coefficient are small. But unlike the transformer with magnetic core, the energy coupling of air-core Tesla transformer is not affected by the saturation of magnetic materials [14]. In addition, the structure of air-core transformer is much simpler. Due to these advantages, air-core Tesla transformer could be applied as boosting devices in repetitive pulse generators.

There are two structures of air-core Tesla transformer: spiral type and strip type. Compared with the strip type, the spiral type transformer has simpler structure, smaller secondary turn-to-turn capacitance and higher turn-ratio [16-18]. A repetitive pulse generator usually requires high average power, which means the switching device should operate on high switching speed with low switching loss. And for a high turn-ratio Tesla transformer,

Manuscript received on 30 September 2014, in final form 9 February 2015, accepted 10 February 2015.

DOI 10.1109/TDEI.2015.004976

the output voltage can reach high amplitude under low primary voltage, so that the semiconductor devices, such as thyristors or IGBTs, can be applied as the primary switch [19]. Therefore, the spiral air-core Tesla transformer combined with semiconductor switching device is feasible for repetitive pulsed power systems [20].

High peak voltage, high repetition rate and high energy efficiency are the most concerned performance in a repetitive pulsed power generator. The output performance of an air-core transformer is mainly related to its double-resonance circuit. When operating on the double-resonance state, where the primary circuit and the secondary circuit have the same intrinsic frequency, an air-core Tesla transformer can attain the maximum energy efficiency and high voltage in theory [21]. Tuning ratio is an important factor which is related to both the output voltage and the energy efficiency. Moreover, when the tuning ratio is changed, the turn-off moment of the primary switch may change too. As a result, the resonant output performance may be different. In summary, researching the resonant charging and tuning effects of air-core Tesla transformer has great significance for its application in repetitive pulsed power systems.

Owing to the background above, this paper focuses on the resonant output performance of spiral air-core Tesla transformer. Aiming at high repetitive performance, the resonant charging and tuning characteristics of spiral Tesla transformer are analyzed. Based on the resonant charging model, the mathematical expressions of secondary voltage, primary current and its maximum rise-rate are deuced. The varying rules of the secondary voltage and energy efficiency are analyzed under different tuning ratios. For experimental study, a spiral air-core Tesla transformer prototype is developed; its circuit parameters are measured and calculated. The tuning ratio of the prototype is adjusted by changing its primary capacitance and secondary capacitance. Combining theory with experiments, the effects of tuning ratio on secondary voltage, primary current and energy efficiency are discussed. Afterwards, the operating mode with suitable output voltage and energy efficiency is selected for repetitive operation.

2 ANALYSIS OF THE RESONANT OUTPUT BASED ON DOUBLE RESONANCE CIRCUIT

2.1 RESONANT CHARGING CHARACTERISTIC

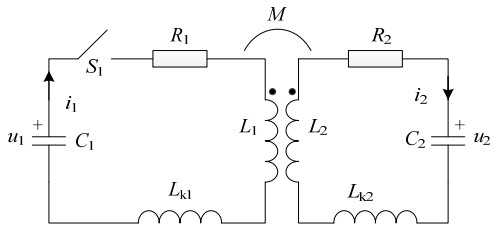

Figure 1. Double resonance circuit of air-core Tesla transformer.

Figure 1 shows the equivalent double resonance circuit of air-core Tesla transformer. C_1 is the primary capacitance. L_1 and R_1 are the equivalent inductance and resistance of the primary circuit, respectively. M represents the mutual inductance. L_{k1} denotes the stray inductance of the primary side. The corresponding circuit elements of the secondary side are marked up as C_2, L_2, R_2 and L_{k2}. At the initial time, the voltage on C_1 is charged to U_1.

k_{eff} is defined as the coupling coefficient between the primary and the secondary winding. ω_{01} and ω_{02} are the angular resonance frequencies of the uncoupled primary and secondary circuits, respectively. The expressions are:

$$k_{eff}^2 = \frac{M^2}{\left(L_1 + L_{k1}\right)\left(L_2 + L_{k2}\right)}, \quad \omega_{0i}^2 = \frac{1}{\left(L_i + L_{ki}\right)C_i} \tag{1}$$

By referring to the reported researches [20], when R_1 and R_2 are ignored, the expressions of the secondary voltage u_2 and the primary current i_1 are presented as:

$$u_2(t) = U_1 k_{eff} e^{-t/T} \sqrt{\frac{L_2 + L_{k2}}{L_1 + L_{k1}}} f_u \tag{2}$$

$$i_1(t) = -U_1 C_1 \omega_1 \frac{x_-^2\left(x_+^2 - 1\right)}{x_+^2 - x_-^2}\left[\sin\omega_1 t + \frac{x_+\left(1 - x_-^2\right)}{x_-\left(x_+^2 - 1\right)}\sin\omega_2 t\right] \tag{3}$$

where T is the time constant of the primary side, x_+ and x_- are the solutions of the circuit equations:

$$x_\pm^2 = \frac{1+\alpha}{2\alpha\left(1 - k_{eff}^2\right)}\left[1 \pm \sqrt{1 - \frac{4\alpha\left(1 - k_{eff}^2\right)}{\left(1+\alpha\right)^2}}\right] \tag{4}$$

In Equation (3), $\omega_1 = x_+ \cdot \omega_{01}$, $\omega_2 = x_- \cdot \omega_{01}$. In Equation (4), α is defined as the tuning ratio of the double resonance circuit which is equal to $\omega^2_{02}/\omega^2_{01}$. If α is equal to 1, which means the ideal resonance of the primary and the secondary circuits. The expression of f_u is:

$$f_u = \frac{\alpha\left(\cos\omega_1 t - \cos\omega_2 t\right)}{\sqrt{\left(1+\alpha\right)^2 - 4\alpha\left(1 - k_{eff}^2\right)}} \tag{5}$$

Existing researches pointed out that, when k_{eff} >0.8, $(u_2)_{\max}$ can be achieved at the first peak of u_2. And when k_{eff} ranges from 0.5 to 0.7, $(u_2)_{\max}$ will appear at the second peak of u_2 [16, 17]. Without the magnetic core, the coupling coefficient of the air-core Tesla transformer is usually delivering up to 0.5-0.8. k_{eff} of 0.6 is recommended for air-core Tesla transformers [18].

When the transformer operates on the resonant state, i.e., $\alpha = 1$, equation (3) can be simplified as:

$$i_1(t) = \frac{-U_1 C_1 \omega_1}{2}\left[\sin\omega_1 t + \sqrt{\frac{1 - k_{eff}}{1 + k_{eff}}}\sin\omega_2 t\right] \tag{6}$$

Because ω_1>ω_2, the primary current i_1 will reach its peak value $(i_1)_{\max}$ when $sin(\omega_1 t)$ is equal to 1. Then the expression of $(i_1)_{\max}$ is:

$$\left(i_1\right)_{\max} = \frac{-U_1\sqrt{C_1}}{2\sqrt{\left(1 - k_{eff}\right)\left(L_1 + L_{K1}\right)}}\left[1 + \sqrt{\frac{1 - k_{eff}}{1 + k_{eff}}}\sin\left(\frac{\pi}{2}\sqrt{\frac{1 - k_{eff}}{1 + k_{eff}}}\right)\right] \tag{7}$$

By taking the derivative of Equation (6), the maximum rise-rate of primary current, $(di_1/dt)_{\max}$, can be expressed as:

$$\left(\frac{di_1}{dt}\right)_{\max} = \frac{U_1}{\left(1 - k_{eff}^2\right)\left(L_1 + L_{K1}\right)} \tag{8}$$

Considering the safety and the lifetime of semiconductor device, $(i_1)_{\max}$ and $(di_1/dt)_{\max}$ should not be too high. As

shown in equations (7) and (8), since U_1 is fixed, $(i_1)_{max}$ is in proportional to $\sqrt{C_1}$, and both $(i_1)_{max}$ and $(di_1/dt)_{max}$ are inversely proportional to (L_1+L_{k1}). And both $(i_1)_{max}$ and $(di_1/dt)_{max}$ are related to k_{eff}. For a constructed Tesla transformer, its primary and secondary inductances are fixed. So k_{eff} is supposed to be unchanged in most cases. Then $(i_1)_{max}$ and $(di_1/dt)_{max}$ can be simplified as:

$$(i_1)_{max} = \gamma U_1 \sqrt{C_1} \tag{9}$$

$$(di_1/dt)_{max} = \lambda U_1 \tag{10}$$

According to equations (7) and (8), γ, λ can be measured and calculated by experiments under low primary voltage.

2.2 TUNING CHARACTERISTIC

Tuning ratio is another important factor which affects the resonant output performance of Tesla transformer. α of 1 is assumed in above analysis. Although α of 1 is more beneficial for energy efficiency, the maximum output voltage is not achieved. In practice, α is adjusted according to actual situation. For example, the well known accelerator Sinus-700, which can operate on high repetition rate, its tuning ratio is 1.36 [9].

As what mentioned, k_{eff}, (L_1+L_{k1}), (L_2+L_{k2}) are supposed to be unchanged for a real Tesla transformer. Thus, the tuning ratio can be adjusted by changing the primary and the secondary capacitance in practice. Then $(u_2)_{max}$ can be presented as:

$$(u_2)_{max} = U_1 k_{eff} \sqrt{\frac{L_2 + L_{k2}}{L_1 + L_{k1}}} F_u \tag{11}$$

where F_u is the maximum value of $|f_u|$.

According to equation (11), when the charging voltage U_1 remains the same, $(u_2)_{max}$ is only determined by f_u. According to equation (5), when k_{eff} remains the same, f_u is a function of t, α and ω_{01}.

Generally speaking, the first and the second amplitude of u_2 are practical, because the first amplitude has short peak-time and the second one has high amplitude. The amplitudes after the second one are usually not in application. Equation (5) is conducted for mathematical analysis in Matlab. The primary capacitance and inductance of air-core Tesla transformer are at the μH or μF level as usual. So ω_{01} is about tens of kHz. ω_{01} can affect the peak-time of f_u, but it does not have effect on the peak value of f_u. Suppose ω_{01} is 80 kHz and k_{eff} is 0.6 in mathematical analysis. When α changes, the simulation curves of f_u are shown in Figure 2.

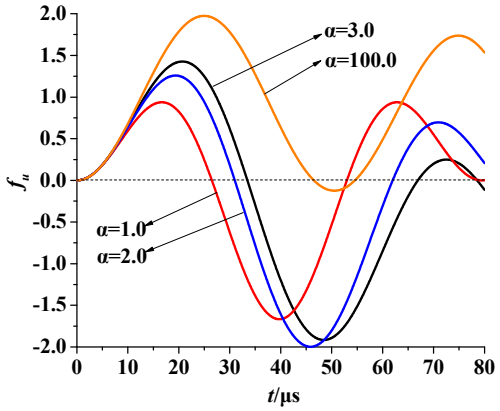

Figure 2. Simulated curves of f_u under different tuning ratios.

Figure 2 shows that the first amplitude of f_u increases gradually as α increases. But the second amplitude of f_u first increases and then decreases. Compared with the other three curves, the second amplitude of f_u with α of 2 is higher. The second amplitude of f_u decreases when α >2.0, which reveals that the main energy storage is transferred from the secondary amplitude to the first amplitude. Otherwise, the curve corresponding to α of 100 indicates that finally the first amplitude may grow very close to its limitation.

According to the calculation results of Matlab, when α=2.086, the second peak of f_u can reach maximum value F_u under k_{eff} of 0.6. In addition, as k_{eff} increases, the corresponding α for f_u to reach F_u will decrease slightly. The theoretical values of α when f_u reaches F_u under different values of k_{eff} are listed in Table 1.

Table 1. Calculation results of α under different k_{eff}.

k_{eff}	0.50	0.52	0.54	0.56	0.58	0.60
α	2.134	2.125	2.116	2.107	2.093	2.086
k_{eff}	0.62	0.64	0.66	0.68	0.70	0.72
α	2.074	2.065	2.052	2.042	2.031	2.022

As Table 1 shows, as k_{eff} ranges from 0.5 to 0.7, the theoretical value of α decreases from 2.134 to 2.031. Hence, air-core Tesla transformer with its tuning ratio $\alpha \approx 2.0$ can get high voltage output in theory.

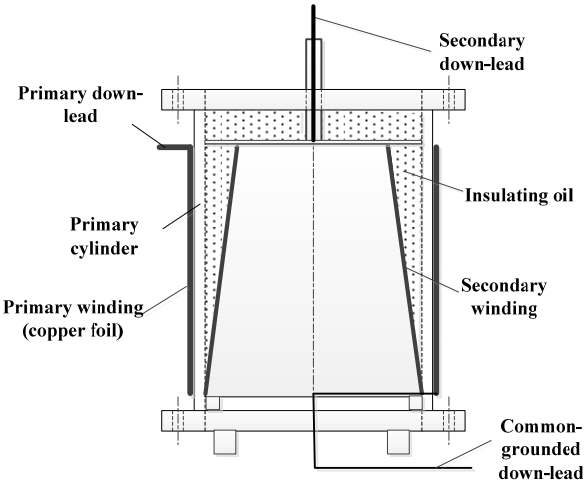

Figure 3. Structure of air-core Tesla transformer prototype.

3 PROTOTYPE FOR EXPERIMENTS

3.1 STRUCTURE OF PROTOTYPE

A spiral air-core Tesla transformer prototype is designed and constructed for experimental study. The overall structure of the prototype is shown in Figure 3. The primary cylinder of the prototype is made of thick plexiglass. And the primary winding is made of 0.2-mm thickness wide copper foil, to reduce the primary resistance. There are 3 turns of primary winding for improving the coupling coefficient and to reduce the maximum rise-rate of the primary current. The touching side of the copper foil is covered by high-performance insulating films to ensure the turn-to-turn insulation. The secondary winding support is made of epoxy sheet of 1 mm

thickness. To strengthen the insulation of the secondary winding, its structure of winding supporter is conical. The secondary winding is made of 0.22 mm polyester-enameled wire, which is tightly wound on the framework. The secondary winding is fixed to the upside of bottom flange of the primary cylinder. The top of secondary winding is covered by a plexiglass plate. The high voltage terminal comes across the cover plate. The primary and secondary winding are connected to the common ground. The space between primary and secondary winding is filled with insulating oil and sealed.

The main structure's parameters after assembly are shown in Table 2, where l is the winding height, r_p is the radius of the primary cylinder, r_{s1} and r_{s2} are the smallest and largest diameter of the secondary conical winding supporter respectively, N_1, N_2 are the turns number of the primary and the secondary winding respectively.

Table 2. Main structure's parameters of the prototype.

Parameters	$2r_{s1}$ (mm)	$2r_{s2}$ (mm)	l (mm)	r_p (mm)	N_1	N_2
Values	280	380	400	200	3	1200

3.2 ELECTRICAL PARAMETERS

The coupling coefficient is the key parameter of air-core Tesla transformer. The primary inductance (L_1+L_{k1}) can be measured when the secondary side is open circuit. And the primary leakage inductance L_{s1} can be measured when the secondary side is short circuit. For the same method, (L_2+L_{k2}) and L_{s2}, can also be measured when the primary side is open circuit and short circuit, respectively [22, 23]. Then the corresponding coupling coefficients of k_{e1} and k_{e2}, can be calculated as following expression:

$$k_{e1} = \sqrt{1 - \frac{L_{s1}}{L_1 + L_{k1}}}, \quad k_{e2} = \sqrt{1 - \frac{L_{s2}}{L_2 + L_{k2}}} \tag{12}$$

The measuring results are listed in Table 3. It is seen that k_{e1} and k_{e2} are very close. So k_{eff} of 0.6 is assumed.

Table 3. Measurement and calculation results of the windings.

Parameters	$L_1 + L_{k1}$ (μH)	L_{s1} (μH)	k_{e1}	$L_2 + L_{k2}$ (mH)	L_{s2} (mH)	k_{e2}
Values	2.89	1.78	0.62	302.42	193.55	0.60

4 EXPERIMENTAL ANALYSIS OF DOUBLE RESONANT PERFORMANCE

4.1 RESONANT CHARGING PERFORMANCE UNDER DIFFERENT CHARGING VOLTAGE

The charging voltage, primary capacitors and secondary capacitors are changed for researching the resonant charging and tuning performance. The primary capacitor C_1 may be made of 2 or 4 metalized film capacitors in parallel. And the measured capacitances of C_1 are 20.3 μF and 41.6 μF, respectively. The secondary capacitor C_2 can consist of 10 or 20 ceramic capacitors in series. The nominal value of each one is 2.4 μF. The measured capacitances of C_2 are 240.0 pF and 120.6 pF, respectively.

As what mentioned, k_{eff} is considered to be unchanged in the following experiments. According to Equation (2), the secondary voltage u_2 is in proportion to the charging voltage U_1 when C_1 and C_2 remain the same. When C_1 is 41.6 μF, and C_2 is 120.6 pF, the waveforms of secondary voltage u_2 under different U_1 are shown in Figure 4.

Seen in Figure 4, the waveforms under different U_1 have the same varying trend. And $(u_2)_{max}$ is in proportion to U_1, which is consistent with Equation (11). When U_1 is 500 V, u_2 reaches about -180kV at its second peak. It means the prototype can achieve a 360 peak transfer ratio when the turn-ratio is 3:1200. The utilization rate of the winding turns is up to 90%, which is close to the magnetic-core transformer, and is higher than 54% proposed in [23].

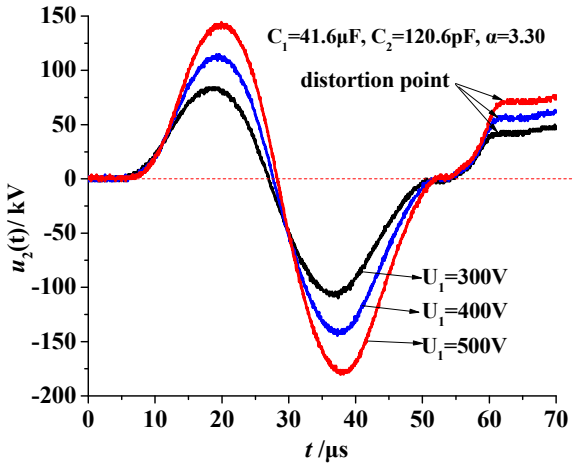

Figure 4. Waveforms of secondary voltage u_2 under different charging voltage U_1.

Semiconductor device S_1 will turn off after the zero-crossing point of i_1 in several microseconds [19]. The turn-off action will cause the distortion on the voltage waveform. The waveform of u_2 distorts after reaching its second peak in Figure 4. It indicates that the turn-off actions of S_1 has no effect on the resonant performance.

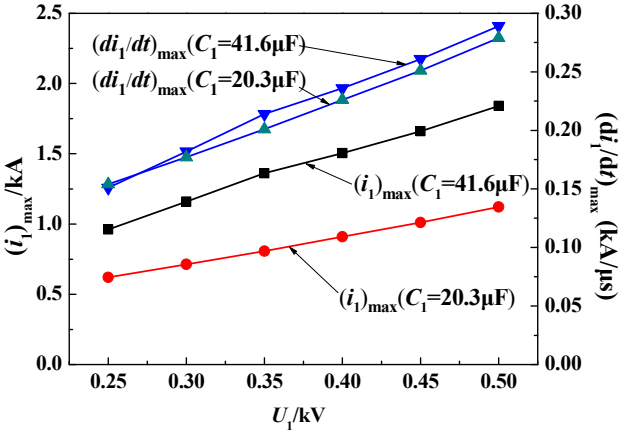

Figure 5. Measurement and calculation results of $(i_1)_{max}$ and $(di_1/dt)_{max}$ under different values of C_1 and U_1.

Equations (9) and (10) present the approximate calculation method of $(i_1)_{max}$ and $(di_1/dt)_{max}$. When C_2 remains 120.6 pF, the measurement and calculation results of $(i_1)_{max}$ and

$(di_1/dt)_{max}$ under different values of C_1 and U_1 are shown in Figure 5. The value of $(di_1/dt)_{max}$ was calculated according to the method reported in [19], that is :

$$(di_1/dt)_{max} = \frac{2}{\pi} \cdot \frac{(i_1)_{max}}{t_m} \quad (13)$$

where t_m is the time of $i_1(t)$ to reach $(i_1)_{max}$.

Equation (7) indicates that $(i_1)_{max}$ is in proportion to $\sqrt{C_1}$, which is verified by the results in Figure 5. When C_1 is 41.6μF, the corresponding curve has larger $(i_1)_{max}$ than another one. Equation (8) indicates that C_1 has no effect on $(di_1/dt)_{max}$. However $(di_1/dt)_{max}$ for two values of C_1 still has a tiny deviation. There are two reasons to explain the deviation. Firstly, equation (8) is an approximate calculation for $(di_1/dt)_{max}$. The circuit resistance, the turn-on resistance of thyristor and other factors are not considered when equation (8) is deduced. When i_1 changes, these ignored factors may have some effects on the calculation result of equation (8). Secondly, k_{eff} is supposed to be unchanged as the prototype is constructed. However, air-core Tesla transformer couples energy by the electromagnetic field of i_1. When i_1 increases, k_{eff} may increase slightly. As a result, $(di_1/dt)_{max}$ will be larger.

According to equations (9), (10) and the measurement results in Table 3, the value of γ and λ for the prototype is -629.47 and 540.66 respectively. When C_1 is 41.6 μF and U_1 is 0.5 kV, the calculation result of $(i_1)_{max}$ is 2.03 kA, and the measurement result in Figure 5 is 1.84 kA. The calculation result of $(di_1/dt)_{max}$ according to Equation (9) is 0.27 kA/μs, the measurement result is 0.29 kA/μs. There are still deviations between calculation results and measurement results. These deviations indicate that equations (9) and (10) are approximate equations. The approximate calculation results can be a reference for insulating design, or for designers to select semiconductor devices of the primary side.

4.2 TUNING PERFORMANCE UNDER DIFFERENT PRIMARY AND SECONDARY CAPACITANCES

To improve the resonant performance, good design to enhance the coupling between the primary and the secondary winding is a solution [21]. But changing the tuning ratio α, is more convenient and practical for a real transformer. (L_1+L_{k1}), (L_2+L_{k2}) and k_{eff} are still considered to be unchanged. The tuning ratio α is adjusted by changing the primary and the secondary capacitance. And the charging voltage U_1 on C_1 remains 0.5 kV in tuning experiments.

The measured waveforms of the secondary voltage u_2 under different C_1 and C_2 are shown in Figure 6. For the convenience of analysis, the corresponding tuning ratios with different capacitances are marked in Figure 6, too.

According to the waveforms in Figure 2 and the data in Table 1, the first amplitude of u_2 will increase when α increases. And the secondary amplitude will reach the maximum value when $\alpha \approx 2.0$. Seen in Figure 6, the curve corresponding to α of 3.30 has higher first amplitude than the other curves, which is consistent with the theory. It means increasing α is an effective way to get higher voltage output when the first amplitude is applied in practice. Different from

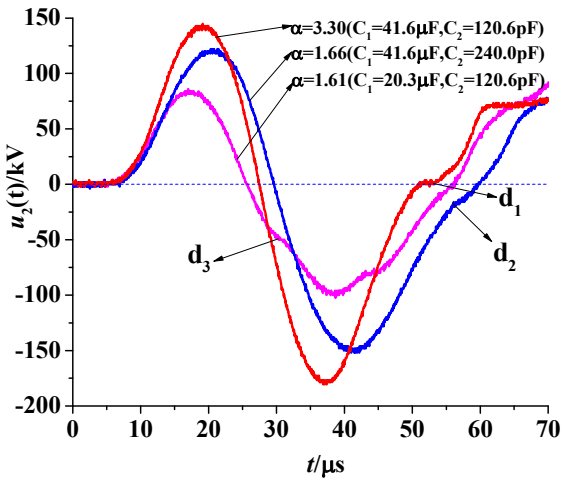

Figure 6. Measured waveforms of u_2 under different C_1 and C_2 (i.e. tuning ratios).

Figure 2, when α is 3.30 in Figure 6, the secondary amplitude is still increasing.

The difference may be caused by two reasons. Firstly, the simulation of f_u did not consider the resistance and the stray parameters of the primary circuit and the secondary circuit. However in actual situation, the energy loss on the resistance and stray parameters will lower the output. Secondly, the energy storage in the primary side increases with the increase of C_1. The curve corresponding to α of 3.30 has larger C_1. So more energy will be transferred to the secondary side, therefore u_2 is still rising. It can be inferred that, α >2.0 is needed to achieve maximum secondary amplitude in actual situation.

Comparing the curve corresponding to α of 1.61 with the curve corresponding to α of 1.66, they have almost the same α. So their amplitudes will be very close in theory. However, the curve corresponding to α of 1.66 has greater voltage amplitude. There are also two reasons to explain the difference. Firstly, the curve corresponding to α of 1.66 has larger C_1, more energy will be transferred to the secondary side. Otherwise larger i_1 may also be helpful to improve the output. Secondly, the distortion points of the curves are different. When C_1 is 41.6 μF, the distortion points d_1 and d_2 appear after the secondary amplitude. So the distortions have no effect on the output. But when C_1 is 20.3 μF, the distortion point d_3 appears before the secondary amplitude, the distortion will lower the output.

Seen in Figure 6, the curve corresponding to α of 1.66 is between the other two curves. It can be inferred that, changing C_1 has greater effect than changing C_2. Because when C_1 remains the same, i_1 changes a little under different C_2. Hence the value of C_2 is usually adjusted after C_1 is fixed in actual situation.

As what mentioned, the turn-off action of S_1 will cause the distortion on the voltage waveform, like d_1 , d_2 and d_3 in Figure 6. In order to investigate the effect of the turn-off moment of the primary semiconductor switch in Figure 6, the corresponding waveforms of i_1 with different C_1 and C_2 are measured in Figure 7.

Observing the turn-off moments d_1, d_2, d_3 of the thyristor in Figure 6 and Figure 7, the turn-off moment can be affected by C_1 and α.

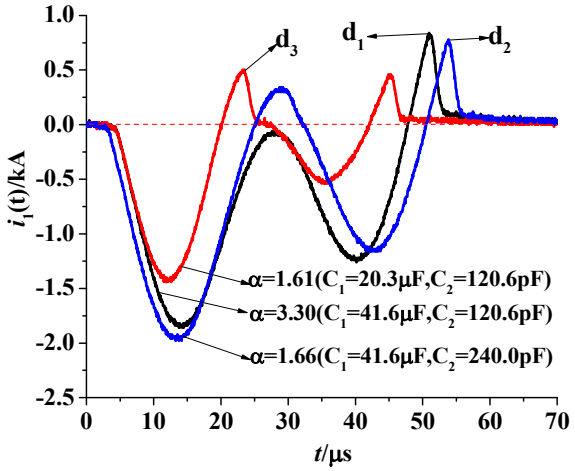

Figure 7. Measured waveforms of the primary current i_1 with different C_1 and C_2 (i.e. tuning ratios).

Firstly, the distortion point d_3 appears before d_2 although they have nearly the same α. Because larger C_1 makes i_1 has longer peak-time, then the second amplitude of i_1 will delay, so that the turn-off moment of the thyristor will delay too. However, considering the withstanding voltage and turn-on current of the primary devices, the increase of C_1 should be limited.

What's more, when α is 1.66, the inverse current cannot cause the turn-off action of the primary switch. It indicates that the thyristor cannot turn off until the inverse current reaches a certain value. When the first peak of i_1 is larger, the needed inverse current will be larger too. This is a common characteristic of semiconductor device. That's why d_2 appears much later than d_3.

Secondly, the distortion points d_1 and d_2 are close because of the same C_1, and they have no effect on the output voltage. The difference is, when α is 3.30, the secondary amplitude is still negative. But the secondary amplitude of another curve has turned positive at about 25 μs. Because larger α will lower the secondary amplitude of i_1, then the zero-crossing point may delay. Otherwise, when α is 1.66, i_1 is not cut off at its first zero-crossing point.

In conclusion, increasing C_1 or α may benefit to delay the turn-off moment of primary switch. The increase of C_1 can delay the second amplitude of i_1. The increase of α can lower the second amplitude of i_1, then the zero-crossing point may appear after the second amplitude.

4.3 ANALYSIS ON ENERGY EFFICIENCY

Energy efficiency η is an important parameter to evaluate the resonant performance, especially in repetitive mode. In practice $(u_2)_{max}$ is usually applied as the output value. Therefore η can be expressed as:

$$\eta = C_2 (u_2)_{max}^2 / C_1 U_1^2 \qquad (14)$$

As the charging voltage U_1 remains 0.5 kV, η is determined by C_1, C_2 and $(u_2)_{max}$. The calculation results of η under different C_1 and C_2 are listed in Table 4.

Comparing the first line with the second line in Table 4, when C_1 remains the same, α is nearer to 1, η will be higher. The same result appears when comparing the third line with the fourth line. The comparing results are consistent with the theory of air-core Tesla transformer.

Comparing the second line with the third line in Table 4, α in these lines are nearly the same, they should have close η in theory. Actually η is much higher in the fourth line, because C_1 is larger, then i_1 is larger, the energy coupling may strengthen as what mentioned.

Table 4. Energy efficiency under different primary and secondary capacitances.

C_1 /μF	C_2 /pF	α	$(u_2)_{max}$ /kV	η
20.3	240.0	0.81	-98.0	45.42%
20.3	120.6	1.61	-119.0	33.65%
41.6	240.0	1.66	-148.6	50.96%
41.6	120.6	3.30	-180.0	37.57%

Otherwise, η reaches 50% in the third line, which is a high value for air-core Tesla transformer. It can be inferred that, if α is closer to 1.0, η will be even higher. But the output voltage will be lower at the same time.

4.4 RESONANT OUTPUT PERFORMANCE IN REPETITIVE MODE

Figure 8 shows the circuit for repetitive operation based on air-core Tesla transformer, where *DC* denotes an DC power source, C_0 and L_0 constitutes a *LC* resonant charging unit, S_0 is the charging switch. To ensure high charging speed, C_0 should be larger than $10C_1$, and C_0 is 1.0 mF in this circuit. C_0 is charged by the DC power source, u_0 is the voltage on C_0. S_1 is the discharging switch. Semiconductor devices such as thyristors or IGBTs are recommended to applied as S_0 and S_1 for improving repetitive operation ability. The voltage on C_2 is measured by a probe of Tektronix P6015A, the primary current is measured by a sensor of Pearson 110.

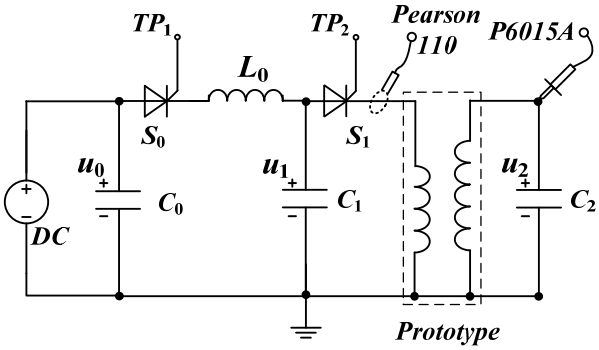

Figure 8. Circuit for repetitive operation based on air-core Tesla transformer.

When S_0 turns on, C_1 is charged complete in a short time. Then S_1 turns on, C_1 discharges through the primary winding. By the coupling of the transformer, C_2 can obtain a high pulsed voltage. When S_0 and S_1 turn on and turn off alternatively, the voltage on C_2 will be repetitive microsecond pulses. The time sequence and the frequency of the triggering signals TP_1 and TP_2 can be set by a microcontroller unit. According to Figure 6, TP_1 is 60 μs ahead of TP_2 at least. It is recommended that S_0 and S_1 have the same type so that they can be driven by just one chip. In addition TP_1 and TP_2 have

the same frequency, which is the repetition rate, to ensure the time sequences are correct. Considering the power of *DC* and the damping time of u_2, the repetition rate should be limited in 500 Hz.

The voltage amplitude and energy efficiency should be both concerned in repetitive operation. Comparing the waveforms in Figure 6 and the data in Table 4, the operation mode corresponding α of 1.66 is selected for repetitive operation. Figure 9 shows the waveforms of u_0 and u_1 when the repetition rate is 300 Hz.

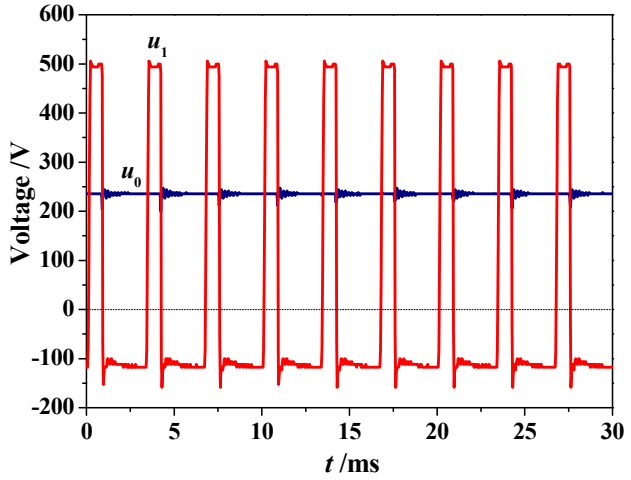

Figure 9. Waveforms of u_0 and u_1 when the repetition rate is 300 Hz.

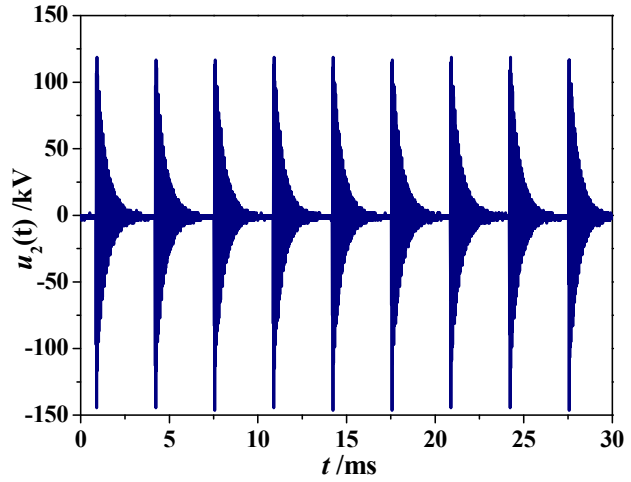

Figure 10. Waveform of microsecond pulses at 300 Hz repetition rate.

Seen in Figure 9, because C_0 is much larger than C_1, u_0 appears as a straight line. In addition C_1 is charged complete in a short time after each discharge. The waveform of u_2 when the repetition rate is 300 Hz is shown in Figure 10.

Seen in Figure 10, the peak value of the pulses are stable at a repetition rate of 300 Hz. And the average value is -140 kV, which has no difference with that in Figure 6. u_0 and α can be higher to get higher u_2. However, the output pulses are bipolar. And the time for u_2 to reach $(u_2)_{max}$ is about 40 μs. Some applications may be limited by the bipolar output or the long peak time [4-6]. Therefore, the output pulses should be compressed to unipolar with fast rise-time for improvement.

5 Conclusions

The technical proposal of combining air-core Tesla transformer with semiconductor devices to generate repetitive high-voltage pulses is feasible and effective. The resonant output performance can be adjusted flexibly by changing the primary capacitance C_1, the secondary capacitance C_2 and the charging voltage U_1. Based on these conditions, this paper can draw the following conclusions:

1) For the resonant charging characteristic, the approximate calculation expressions of maximum primary current and the maximum rise-rate of primary current are deduced. Increasing primary inductance can limit the primary current and its rise-rate effectively. The resonant output voltage and primary current are in proportion to the charging voltage. Large primary current may be helpful to the energy coupling of air-core Tesla transformer.

2) For the tuning characteristic, the first amplitude of the output voltage will increase as the tuning ratio increases. The second amplitude has the theoretical maximum value under a certain tuning ratio. Increasing tuning ratio can lower the second amplitude of primary current, then the turn-off moment of the primary switch will delay. In repetitive mode, the tuning ratio is recommended to range in 1.0-2.0 to achieve high energy efficiency.

3) For repetitive operation, to trigger the charging and discharging switch turn on and turn off alternatively can achieve repetitive operation. It is recommended that two switches have the same type and operate on the same frequency. When C_1 is 41.6 μF, C_2 is 240.0 pF, U_1 is 0.5 kV the prototype can operate on 300 Hz repetition rate stably, and the microsecond pulses has the average peak value of -140 kV.

Acknowledgements

The authors gratefully acknowledge the support of the Open Foundation of State Key Laboratory of Advanced Electromagnetic Engineering and Technology, Grant No. 2014KF002, and Research Fund of China Academy of Engineering Physics, Grant No. 2013AA8032051.

References

[1] H. Akiyama, T. Sakugawa, and T. Namihira, "Industrial applications of pulsed power technology", IEEE Trans. Dielectr. Electr. Insul., Vol. 14, pp. 1051-1060, 2007.

[2] T. Shao, G. S. Sun, P. Yan and S. C. Zhang, "Breakdown phenomena in nitrogen due to repetitive nanosecond-pulse", IEEE Trans. Dielectr. Electr. Insul., Vol.14, pp. 813-819, 2007.

[3] E. L. Neau, "Environmental and industrial applications of pulsed power systems", IEEE Trans. Plasma Sci., Vol. 22, pp. 2-3, 1994.

[4] T. Shao, Y. Yu, C. Zhang, D.D. Zhang and Z. Liu, J. Wang and P. Yan, "Excitation of atmospheric pressure uniform dielectric barrier discharge using repetitive unipolar nanosecond-pulse generator", IEEE Trans. Dielectr. Electr. Insul., Vol.16, pp. 1830-1835, 2010.

[5] T. Shao, D. D. Zhang and Y. Yu, "A compact repetitive unipolar nanosecond-pulse generator for dielectric barrier discharge application", IEEE Trans. Plasma Sci., Vol.38, pp. 1651-1652, 2010.

[6] F. Fukawa, N. Shimomura and T. Yano, "Application of nanosecond pulse power to ozone production by streamer corona", IEEE Trans. Plasma Sci. Vol., 36, pp. 2592–2597, 2008

[7] A. Fridman, A. Chirokov and A. Gutsol, "Non-thermal atmospheric pressure discharges", J. Phys. D: Appl. Phys., Vol. 38, pp. R1-R24, 2005.

[8] S. Pinguet, J. P. Dupéroux, P. Delmote, F. Bieth, and R. Bischoff, "Short-pulse Marx generator for high-power microwave applications", IEEE Trans. Plasma Sci., Vol. 41, pp. 2754-2757, 2013.

[9] G.A. Mesyats, S. D. Korovin, A. V. Gulin, V. P. Gubanov, A. S. Stepchenko, D. S. Grishin, V. F. Landl and P. I. Alekseenko, "Repetitively pulsed high current accelerators with transformer charging of forming lines", Laser Part. Beams, Vol. 21, pp. 197-209, 2003.
[10] G.A. Mesyats, S. D. Korovin, V. V. Rostov, V. G. Shpak and M. I. Yalandin, "The RADAN series of compact pulsed power generators and their applications", Proc. IEEE, Vol. 92, pp. 1166-1179, 2004.
[11] X. X. Song, G. Z. Liu, J. C. Peng, J. C. Su, L. M. Wang, X. X. Zhu, Y.F. Pan, X. B. Zhang, W. H. Guo, S. Qiu and W. H. Huang, "A repetitive high-current pulsed accelerator—TPG700," in Proc. 17th Int'l. Conf. High-Power Part. Beams (Xian, China) pp. 75–79, 2008.
[12] V. P. Gubanov, S. D. Korovin and I. V. Pegel, "Compact 1000 PPS high-voltage nanosecond pulse generator", IEEE Trans. Plasma Sci., Vol. 25, pp. 258–265, 2011.
[13] S. O. Macheret, M. N. Shneider and R. B. Miles. "Modeling of air plasma generation by repetitive high-voltage nanosecond pulses", IEEE Trans Plasma Sci., Vol. 30, pp. 1301–1314, 2002.
[14] Z. Yu, Liu J. L, X. B. Cheng and H. B. Zhang, "Output characteristics of a kind of high-voltage pulse transformer with closed magnetic core", IEEE Trans. Plasma Sci., Vol. 38, pp. 1019-1027, 2010.
[15] E. M. M. Cost, "Resonance on coils excited by square waves: explaining Tesla transformer". IEEE Trans. Magn., Vol. 46, pp. 1186-1192, 2010.
[16] J. Luo, B. M. Novac, I. R. Smith and J. Brown, "Fast and accurate two-dimensional modelling of high-current, high voltage air-cored transformers", J. Phys. D: Appl. Phys., Vol.38, pp. 955-963, 2005.
[17] J. Q. Xin, M. J. Li and Q. Kang, "High transformer ratio and conical spiral air-cored pulse transformer", High Power Laser and Particle Beams, Vol. 22, pp. 216-220, 2010 (in Chinese).
[18] M. J. Li, J. Q. Xin, Q. Kang, S. G. Gong and X. Jin, "Development of 800 kV spiral air-cored transformer with high turn ratio", High Power Laser and Particle Beams, Vol. 23, pp. 841-844, 2011 (in Chinese).
[19] L. Li, C. B. Bao, X. B. Feng, Y. Liu and F. C. Lin, "Fast switching thyristor applied in nanosecond-pulse high-voltage generator with closed transformer core", Rev. Sci. Instrum., Vol. 84, pp. 024703-024703-7, 2013.
[20] J. R. Reed, "Designing triple resonance Tesla transformers of arbitrary modal frequency ratio," Rev. Sci. Instrum., Vol. 77, pp. 1–6, 2006.
[21] M. Denicolai, "Optimal performance for Tesla transformers", Rev. Sci. Instrum., Vol.73, pp. 3332-3335, 2002.
[22] A. Lindblom, J. Isberg and H. Bernhoff, "Calculating the coupling factor in a Multilayer coaxial transformer with air core", IEEE Trans. Magn., Vol. 40, pp. 3244-3247, 2004.
[23] B. Juergen and W. K. Johann, "Using Transformer Parasitics for Resonant Converters-A review of the Calculation of the Stray Capacitance of Transformers", IEEE Trans. Industry Appl., Vol.44, pp.223-233, 2008.

Lee Li was born in Hubei province, P.R. China in 1976. He received the Ph.D. degree from the Department of Electronics and Information Engineering, Huazhong University of Science and Technology (HUST), Wuhan, China, in 2006. He is currently an Associate Professor with the College of Electrical and Electronic Engineering, HUST. He is working on and high voltage power engineering, pulsed-power and arc discharge technology. He is a member of the Chinese society for electrical engineering.

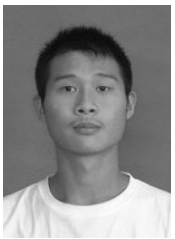

Ma Ning was born in Henan province, China, in 1991. He has been studying for the M.S. degree in the High Voltage Engineering Department, the School of electrical & electronic engineering, Huazhong University of Science and Technology (HUST).

Chen Dehuai was born in Sichuang province, China, in 1968. He received the M.S. degree in electrical and electronic engineering from HuaZhong University of science and technology (HUST) in 2006. He is the corresponding author of this paper. He has been working on pulsed power technology and high voltage engineering in Laser Fusion Research Center in China Academy of Engineering Physics.

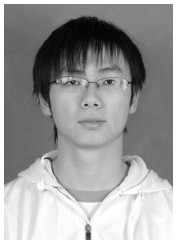

Liu Lun was born in Hubei province, China, in 1985. He has been studying for the M.S. degree in the High Voltage Engineering Department, the School of electrical & electronic engineering, Huazhong University of Science and Technology (HUST).

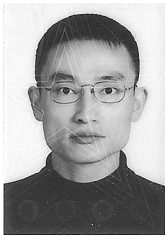

Kang Qiang was born in 1974 in Sichuan province, China. He received the Master degree from Huazhong University of Science and Technology in 1998. He devotes himself to pulsed power research in China Academy of Engineering Physics (CAEP).

Li Mingjia was born in 1977 in Hubei province, China. He received the B.S. and M.S. degrees in high voltage engineering from Chongqing University in 1999 and 2002, respectively. In 2011, he received the Ph.D. degree in nuclear technology and applications in Graduate School of China Academy of Engineering Physics (CAEP). His research interests include high voltage engineering and pulsed power.

Cheng Yong was born in Anhui province, China, in 1990. He has been studying for the M.S. degree in the High Voltage Engineering Department, the School of electrical & electronic engineering, Huazhong University of Science and Technology (HUST).

Yuan Pan received the B.S. degree in electrical engineering from the Huazhong University of Science and Technology, Wuhan, China, in 1955. He is currently a Professor and the Honorary Dean of the College of Electrical and Electronic Engineering, Huazhong University of Science and Technology, where he is also with the Key Laboratory of Nuclear Fusion and Advanced Electromagnetic Technology, Ministry of Education. His main research interests include magnetic confinement nuclear fusion, high-power pulse source technology, superconducting electric power, and pulse power technology.